METALLIC CLUSTERS IN CdI_2 CRYSTALS: ELECTRON MICROSCOPY STUDY AND COMPUTER-BASED ANALYSIS OF THEIR NUMERICAL CHARACTERISTICS

I.M. BOLESTA, R.I. HRYTSKIV, YU.R. DATSIUK, B.M. PAVLISHENKO

Ivan Franko Lviv National University
(107, Tarnavskogo Str., Lviv, Ukraine; e-mail: bolesta@electronics.wups.lviv.ua)

UDC 537.533.35; 004.932

Metallic clusters of cadmium have been revealed in CdI_2 crystals grown from a melt or a gas phase by means of the scanning electron microscopy (SEM) technique. It is shown that, in the former case, the clusters are formed when a composition deviates from the stoichiometric one towards a cadmium content growth. In the latter case, the metallic clusters form fractal structures, whose fractal dimension is $D \approx 1.73$, on the surface of crystals. The algorithms to analyze the cluster structures on the basis of their images are proposed and implemented. This makes it possible to calculate the radii of clusters, intercluster distances, and distribution functions for these parameters. It is demonstrated that there exists a difference in numerical parameters between the clusters formed in crystals grown by different techniques, which points to the differences in the cluster formation mechanisms. The formation of cluster structures on the surface of the crystals grown from a gas phase is simulated in the frame of a diffusion-limited aggregation model. It is concluded that these structures are formed by the particle-cluster mechanism, with the growth centers being inhomogeneous regions of the surface of a crystal.

1. Introduction

Crystals of iodine cadmium belong to a MX_2-type halogenide family with a layered structure which is characterized by a dense hexagonal package of iodine atoms, where a half of octahedral voids is occupied by cadmium atoms. Strong ionic-covalent bonds between cadmium and iodine atoms give rise to the formation of triple layers (or "sandwiches") I–Cd–I, which are considered as the structure unit of a crystal. Three-dimensional crystals are formed by stacking these sandwiches. In this case, each two triple layers are bound by weak van der Waals forces, which brings about an ideal cleavage of CdI_2 along (0001) basal planes.

Separate stacking faults, which exist in a dense atomic package, give rise to a one-dimensional (along the c-axis) structure disordering, whereas their periodic repetition results in the formation of polytypic modifications, the number of which reaches 200 for CdI_2 [1].

The ordered arrangement of triple layers along the c-axis, which corresponds to the hexagonal close package rule, constitutes the $2H$ polytype with unit cell parameters $a = b$=0.428 nm and c=0.686 nm. However, most wide-spread is the four-layered $4H$-CdI_2 structure, whose unit cell contains two triple layers. Therefore, the c-parameter of the $4H$ polytype is twice as greater as that of the 2H one and equals 1.373 nm.

A weak bond between the iodine atoms from the neighboring triple layers leads to the existence of van der Waals gaps in the CdI_2 structure, which are formed by unoccupied octa- and tetrahedral voids. Since the thickness of an I–Cd–I sandwich is 0.342 nm [2], the width of the van der Waals gap in CdI_2 can be calculated from the value of the c-parameter for the $2H$ polytype and is 0.344 nm.

A characteristic feature of CdI_2 is that, irrespective of the growth method and the post-growth heat treatment, it contains overstoichiometric cadmium atoms Cd_i. The investigations show that these atoms are predominantly located in octahedral voids of the van der Waals gaps and can form the chemical bonds with iodine atoms from different sandwiches. This process can be considered as the CdI_2 self-intercalation, and it gives rise to a change in the c-parameter of the crystal lattice [3]. This manifests itself, in turn, in changing the electron spectra [4,5], the frequency of the ^{127}I nuclear quadruple resonance (as a result of a variation of the gradient of an electric field [3]), and has an influence on the nonlinear optical properties [7,8]. It is concluded from the concentration dependences of these effects that the overstoichiometric cadmium atoms can form metallic clusters $(Cd_i)_n$ [3,5]. It should be noted that similar effects were also observed in doped CdI_2 crystals as a result of the localization of impurity atoms in van der Waals gaps [14–19].

The aim of this work is to prove the existence of metallic clusters by making use of the SEM methods and to develop an approach and algorithms of determination

of the quantitative characteristics which can be used to describe the clusters and the structures they form in the CdI_2 crystals with a broken stoichiometry.

2. Crystals for Investigation

The objects of investigation were CdI_2 crystals with a controlled deviation from the stoichiometric composition, which were grown from a melt by the Bridgman–Stockbarger method. The crystals with the concentration of interstitial Cd atoms $N_i = 10^{16}$, 10^{17}, 10^{18}, and 10^{19} cm^{-3} were obtained by means of the introduction of metallic cadmium, whose concentrations were 10^{-4}, 10^{-3}, 10^{-3}, and 10^{-1} mol% respectively, in the melt (the concentration of atoms in CdI_2 is $\sim 10^{22}$ cm^{-3}). Assuming that the Cd_i atoms are uniformly distributed within the lattice, the distance between the overstoichiometric atoms can be estimated from the relation

$$r = N_i^{-1/3} \tag{1}$$

and is 46, 21, 10, and 5 nm, respectively.

Along with these specimens (in what follows – CdI_2-M crystals), the CdI_2 crystals obtained from a gas phase were investigated (in what follows – CdI_2-G crystals). The latters were in the form of thin ($d \gtrsim 10$ μm) plates and had areas of 5–10 mm^2.

3. Microscopic Studies

The investigation of the surface microstructure for the CdI_2 crystals was performed with the use of an JEOL-T220A electron microscope. Freshly cleaved (0001) base planes for the CdI_2-M crystals and "aged" surfaces for the CdI_2-G ones were studied in reflected and elastically scattered electrons. In all the cases, the electron beam energy was 20 keV.

For the CdI_2-M crystals with 0.1 mol% of overstoichiometric Cd, the clusters on the crystal surface are clearly discernible (Fig. 1). Their distribution over a specimen surface is nonuniform; there are regions which do not contain the clusters at all. There exists a correlation between the surface density of clusters and a degree of deviation of the composition from the stoichiometric value: the largest cluster density is observed in the crystals with the highest degree of the composition deviation (0.1 mol %). No regions with a high cluster density are revealed in the crystals with a lower level of doping.

Metallic clusters were also revealed on the surface of the CdI_2-G crystals (see Fig. 1). In all the cases, the

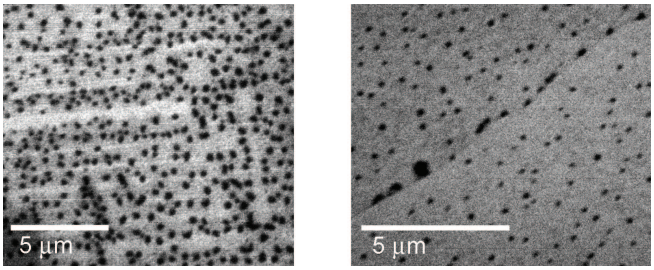

Fig. 1. SEM patterns for clusters on the surface of CdI_2-G (left) and CdI_2-M (right) crystals

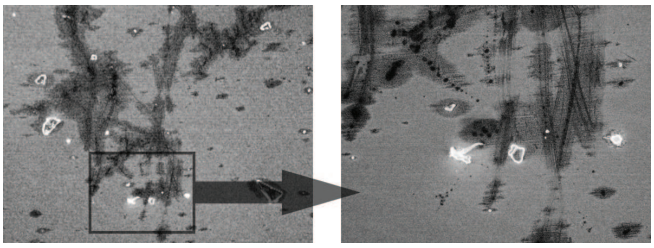

Fig. 2. Self-similarity of the cluster structure on the surface of a CdI_2-G crystal. The image is magnified by 100 (left) and 500 (right) times

clusters on the surface of the CdI_2 crystals form fractal structures. This follows from a self-similarity, which can distinctly be seen at different magnifications (Fig. 2). The fractal dimension of these structures calculated by a box-counting method [21] is $D \approx 1.73$.

The data available in the literature on the microscopic studies of the CdI_2 surface refer only to the crystals obtained from an aqueous solution [1,12,13]. The substeps were revealed on the spirals of growth. These substeps are formed on the (0001) base planes, and the distance between them is a multiple of the a-parameter of the crystal lattice [12]. This distance depends, in turn, on a degree of supersaturation of a solution σ and diminishes with increase in σ, according to the theory of a dislocation growth.

Atomic force microscopy methods made it possible to observe steps, terraces, channel-like hollows, and islets on the surface of CdI_2 crystals [3]. At the same time, the area between these topography elements is atomically flat. It is revealed that the morphology of the CdI_2 surface undergoes changes after the crystals are kept in air. This phenomenon is associated with the processes of solution and recrystallization which occur on the surface as a result of the absorption of a thin layer of water.

Work [13] provides the evidence of that the exposure of CdI_2 to an electron beam gives rise to the formation

of nanoparticles with a closed cell structure. These are predominantly metallic, since the ratio of the Cd content to the I one is 2 : 1, whereas this ratio equals 1 : 1.5 for the stoichiometric CdI_2. Such a phenomenon is a result of the recrystallization, which is initiated, in turn, by the evaporation under the action of the electron beam.

4. Calculation Technique and Results of Numerical Simulation

To interpret the results obtained by electron microscopic studies, one should look for a way to quantitatively characterize the clusters and the structures they form. Here, we proposed the algorithms of image vectorization, which can give quantitative characteristics for the clusters observed. Consider the vectorization process in more details.

Define a cluster on raster images as an aggregate of elements (image pixels) grouped into the classes characterized by specified parameters which can vary only within the certain limits peculiar to each of the classes. For a graphic BMP standard, the pixel brightness and the distance between pixels were chosen as the grouping parameters.

To measure the cluster characteristics, the image vectorization should be carried out first. The vectorization procedure consists in the conversion of an image into a numerical format which allows its subsequent deep analysis. The first step in this operation is the smoothing of a raster image to eliminate the noise effects, because these will subsequently become evident in the form of separate pixels. In our case, the smoothing procedure was carried out by averaging the brightness of a pixel with respect to that of the neighboring elements, and this was done by means of the discrete convolution of a raster image with Gaussian [11].

The next step in the cluster vectorization, according to the algorithm chosen, is an image binarization. This procedure consists in a grouping of pixels according to whether the brightness parameter belongs to a specified range or not [11]. In its turn, the boundaries of this range specify the number of elements which will eventually be included in clusters and the number of clusters themselves. To define such a range, it is enough to specify the minimal (maximal) brightness value and the so-called brightness threshold. As a result of the binarization, an image is segregated into separate clusters. They can be larger or smaller in size, depending on whether a lower or a higher value of the brightness threshold is chosen. This results in a smaller or greater number of clusters, respectively. Returning to our case, the brightness threshold was chosen in such a way that the number of clusters was as large as possible.

The further step consists in the use of the algorithm of point filtration with the aim to separate those clusters which have a small number of the points of contact on a binarized image.

To clusterize the elements on a binarized image, we used one of the agglomerate algorithms [9,10] which merges a few clusters into a single one, basing on the results of the comparison of intercluster distances with a preset threshold value. At the initial step, each pixel is considered as a separate cluster. The clusters are joined together if the distance between them does not exceed the preset threshold value. This procedure recurs until the distance between all clusters is greater than the threshold value. As a result of the clusterization procedure, a pixel array is ascribed to each the cluster.

Proceeding from such a representation of the data, the clusters were approximated by circles with radius R which was defined as

$$R = \sqrt{\frac{S}{\pi}}, \tag{2}$$

where S is the cluster area calculated from the number of elements which form the image. The coordinates of the center of such a circle were defined as the average values of pixel coordinates of the array for each cluster. In a similar way, the distance R_c to a nearest neighbor was defined as the smallest of the distances to all other clusters.

The analysis of the cluster structures on the surface of the CdI_2 crystals was carried out with the use of the techniques described above. The numerical parameters which characterize the clusters and their distribution on the crystal surface are presented in the Table.

An important characteristic is the cluster radius distribution function $F(R)$. The knowledge of it makes it possible to calculate the number of clusters N_c, whose radii are between R_1 and R_2:

$$N_c = N \int_{R_1}^{R_2} F(R)dR, \tag{3}$$

where N is the total number of clusters.

Measured characteristics for the cluster structures: $\bar{R}$ is the average cluster radius, σ_R the root-mean-square deviation of R, $\bar{R}_c$ the average distance to the nearest neighbor, σ_{R_c} the root-mean-square deviation of R_c

Crystal	$\bar{R}$, μm	σ_R, %	$\bar{R}_c$, μm	σ_{R_c}, %
CdI_2-M	0.085	31	0.622	31
CdI_2-G	0.122	36	0.489	25

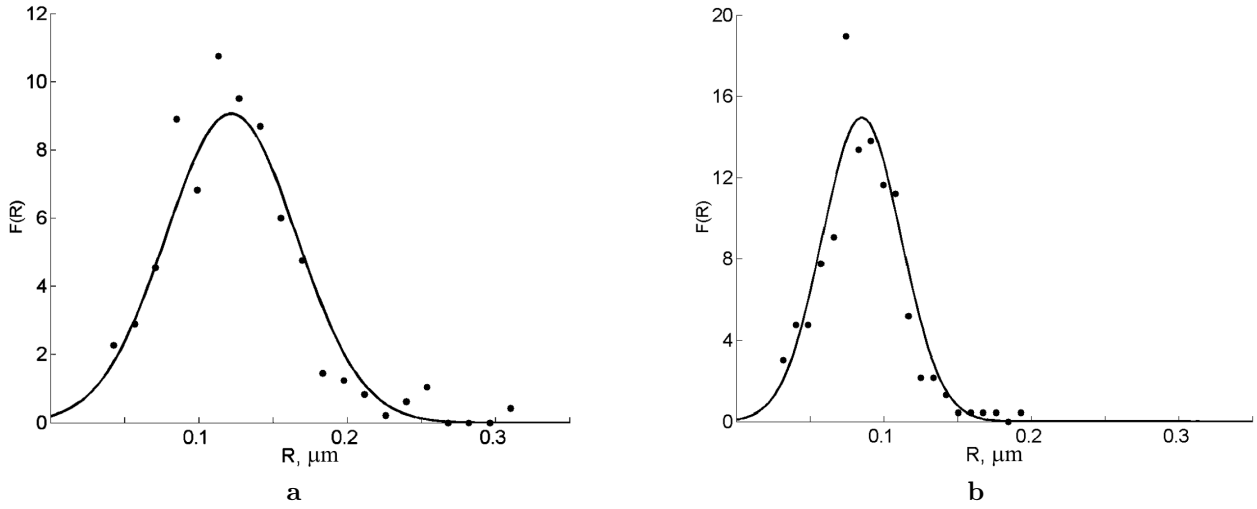

Fig. 3. Cluster radius distribution for the patterns on the surface of the CdI_2-G (*a*) and CdI_2-M (*b*) crystals: points – the data obtained by means of the image processing, solid line – the corresponding Gaussian distribution

The data on the distribution of clusters over radii, which were derived from the processing of the SEM images obtained experimentally, are shown in Fig. 3,*a,b* for the CdI_2-G and CdI_2-M crystals, respectively.

To carry out the calculations, the whole range of the radius values was divided into equal intervals and the number of the clusters, whose radii were within a certain interval, was counted. The normalized values obtained in such a way are shown by points. The solid curves in Figs. 3 and 4 show the Gaussian distribution calculated according to the formula

$$F(R) = \frac{1}{\sqrt{2\pi}\sigma} \exp\left[-\frac{(R-\bar{R})^2}{2\sigma^2}\right], \tag{4}$$

where $\bar{R}$ is the average value and σ is the variance. These two parameters were taken from the statistical computations (see the Table). It is clear that the cluster radius distribution functions obtained in different ways well correlate with each other.

Similar distribution functions were obtained for R_c for the cluster structures on the surfaces of the CdI_2-G and CdI_2-M crystals.

Let us analyze the obtained results and carry out their comparison. First, we calculate the number of the atoms which form a cluster. The cluster radius is related to the number of particles contained in it,

$$R = r_{\mathrm{WS}} N^{1/3}, \tag{5}$$

where r_{WS} is the radius of a Wigner–Seitz cell. It can be calculated as

$$r_{\mathrm{WS}} = \left(\frac{3}{4\pi n}\right)^{1/3}, \tag{6}$$

where n is the concentration of free electrons [24]. For cadmium, $n = 9.27\times10^{22}$ cm^{-3} and, thus, $r_{\mathrm{WS}} = 1.37$ Å. As a result, the average number of atoms in a cluster is $\approx 2.4 \times 10^8$ for the CdI_2-M crystals and $\approx 7.1 \times 10^8$ for the CdI_2-G ones.

The data presented in the Table show that the intercluster distance is far greater than the cluster radius. At the same time, this distance is comparable with a wavelength of visible light.

Let us compare the cluster sizes with the electron free path. It is known [25] that the electron free path in metals does not exceed 20 nm at room temperature and thus is 4–6 times less than the cluster radius. Another natural scale is the Fermi wavelength

$$\lambda_{\mathrm{F}} = \frac{2\pi}{k_{\mathrm{F}}}, \tag{7}$$

where the Fermi wavenumber k_{F} can be found from the expression [24]

$$k_{\mathrm{F}} = \sqrt[3]{3\pi^2 n}. \tag{8}$$

For cadmium, $k_{\mathrm{F}} = 1.4\times10^8$ cm^{-1}, and, thus, the Fermi wavelength $\lambda_{\mathrm{F}} = 0.45$ nm, which is again less than the cluster radius.

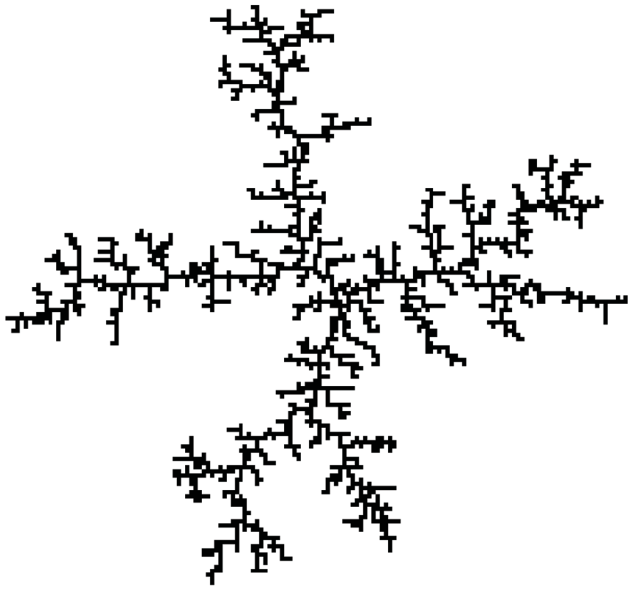

Fig. 4. Fractal structure (2000 elements) simulated within the particle-cluster model

The analysis of the data of the Table also demonstrates a difference in the cluster radii R between the CdI_2-M and CdI_2-G crystals. This points to the differences in the cluster formation mechanisms. In the case of the CdI_2-M crystals, the clusters are formed in the crystal bulk as a result of the diffusion of non-stoichiometric cadmium atoms and their subsequent merging into aggregates in the van der Waals gaps. In another case, however, the clusters are formed on a surface, and this is likely to occur as a result of the surface diffusion of cadmium atoms which are formed upon the dissociation of CdI_2 molecules at high temperatures of the crystal growth.

With the aim to explore the formation mechanism for fractal cluster structures on the surface of CdI_2-G crystals, two computer-based models of growth are considered to be suitable: the particle-cluster model [22] and the cluster-cluster [23] one. In both the models, the clusters are formed by means of the merging of smaller objects (atoms, subclusters). The main difference between these models is that the former model presumes the existence of a growth center (a nucleus), whereas the latter one considers all structural elements as equivalent. Figure 4 shows the model of a fractal structure which consists of 2000 elements and is formed according to the particle-cluster algorithm. Its fractal dimension is $D \approx 1.70$, which is close to the value for the real structure observed on the surface of a CdI_2-G crystal. For this reason, it can be concluded that the formation of clusters and their aggregates occurs around separate centers which can be, as follows from the microscopic studies [2, 12], such peculiarities of a surface relief as grooves, terraces, dips, *etc.*

5. Conclusions

The SEM methods made it possible to prove the existence of metallic cadmium clusters in the CdI_2 crystals grown from a melt and the gas phase. The correlation is found between the features of the cluster formation and a degree of the composition deviation from the stoichiometry. On the surface of the CdI_2-G crystals, the metallic clusters form the structures whose fractal dimension is $D \approx 1.73$.

We have proposed and implemented the algorithms to analyze the images of the cluster structures. These include the primary image processing as well as the algorithms of vectorization, filtration, and calculation of a fractal dimension. This paves the way for the calculations of the numerical parameters of clusters and the structures they form.

It is demonstrated that the radius of the clusters formed on the crystal surface is greater for the CdI_2-G crystals than that for the CdI_2-M ones, which implies the difference in the mechanisms of their formation. It is shown that there is a good agreement between the fractal dimension for the real crystals and those obtained within the frame of the particle-cluster model, which points to a likely mechanism of their formation.

1. *Wide Bandgap Layered Crystals and Their Physical Properties*, ed. by A.B. Lyskovich (Vyshcha Shkola, L'viv, 1982) (in Russian).
2. Nai-Yu Cui, M.D. Brown, and A. McKinley, Appl. Surf. Sci. **155**, 266 (1999).
3. I.M. Bolesta, I.V. Kityk, V.I. Kovalisko, and R.M. Turchak, Ferroelectrics **192**, 107 (1997).
4. I.M. Bolesta, I.V. Kityk, V.I. Kovalisko, and R.M. Turchak, Ukr. Fiz. Zh. **39**, 1084 (1994).
5. I.M. Bolesta, I.V. Kityk, V.I. Kovalisko, and R.M. Turchak, Radiation Effects and Defects in Solids **137**, 95 (1995).
6. I.M. Bolesta, A.V. Gal'chinskiy, and I.V. Kityk, Fiz. Tverd. Tela **37**, 1536 (1995).
7. I.M. Bolesta, I.V. Kityk, and R.M. Turchak, Fiz. Tverd. Tela **36**, 1632 (1994).
8. I.M. Bolesta, I.V. Kityk, J. Filipecki, and H. Zount, Phys. Status Solidi B **189**, 357 (1995).
9. J.O. Kim, C.W. Mueller, et al., *Factor, Discriminant, and Cluster Analyses* (Finansy i Statistika, Moscow, 1989) (in Russian).

10. M. Jambu, *Classification Automatique pour l' Analysis des Donnees* (Dunod, Paris, 1987).

11. B.V. Anisimov, V.D. Kurganov, and V.K. Zlobin, *The Recognition and Digital Image Pocessing* (Vysshaya Shkola, Moscow, 1983) (in Russian).

12. R. Singh, S.B. Samanta, A.V. Narlikar, and G.C. Trigunayat, J. Cryst. Growth **204**, 233 (1999).

13. N. Sallacan, R. Popovitz-Biro, and R. Tenne, Solid State Sci. **5**, 905 (2003).

14. M. Ollafsson and F. Stenbery, Opt. Materials **25**, 341 (2004).

15. S.A. Pyroga, I.D. Olekseyuk, and O.M. Yurchenko, Ukr. Fiz. Zh. **46**, 735 (2001).

16. O.M. Yurchenko, S.A. Pyroga, and I.D. Olekseyuk, Zh. Prikl. Spektroskop. **68**, 771 (2007).

17. A.V. Gloskovskiy, M.R. Panasyuk, L.I. Yaritskaya, and N.K. Gloskovskaya, Fiz. Tverd. Tela **45**, 390 (2003).

18. M. Terakami, H. Nakagava, K. Fkui, H. Okamura, T. Hirono, Y. Ikemoto, T. Moriwaki, and H. Kimura, J. Phys. Soc. Jpn. **72**, 2128 (2003).

19. M. Terakami, H. Nakagava, K. Fkui, H. Okamura, T. Hirono, Y. Ikemoto, T. Moriwaki, and H. Kimura, J. Luminescence **108**, 75 (2004).

20. B.B. Mandelbrot, *The Fractal Geometry of Nature* (Freeman, New York, 1983).

21. K.J. Falconer. *The Geometry of Fractal Sets* (Cambridge University Press, Cambridge, 1985).

22. T.A. Witten and L.M. Sander, Phys. Rev. Lett. **47**, 1400 (1981).

23. P. Meakin, Phys. Rev. Lett. **51**, 119 (1983).

24. N.W. Ashcroft and N.D. Mermin, *Solid State Physics* (Holt, Rinehart, and Winston, New York, 1976).

25. N.W Ashcroft, Usp. Fiz. Nauk **104**, 519 (1970).

Received 11.07.07.
Translated from Ukrainian by A.I. Tovstolytkin

ЕЛЕКТРОННО-МІКРОСКОПІЧНІ ДОСЛІДЖЕННЯ ТА КОМП'ЮТЕРНИЙ РОЗРАХУНОК ЧИСЛОВИХ ХАРАКТЕРИСТИК МЕТАЛІЧНИХ КЛАСТЕРІВ В КРИСТАЛАХ CdI_2

І.М. Болеста, Р.І. Грицьків, Ю.Р. Дацюк, Б.М. Павлишенко

Р е з ю м е

В роботі методами скануючої електронної мікроскопії виявлено металічні кластери кадмію в кристалах CdI_2, вирощених з розплаву та з газової фази. Показано, що у кристалах, вирощених з розплаву, кластери утворюються за умови порушення стехіометрії у бік збільшення вмісту металічного кадмію. На поверхні кристалів, отриманих з газової фази, металічні кластери формують структури, фрактальна розмірність яких $D \approx 1,73$. Запропоновано та реалізовано алгоритми аналізу кластерних структур на основі їхніх зображень, з допомогою яких визначено радіуси кластерів, відстані між ними та функції розподілу цих величин. Встановлено, що числові параметри кластерів є різними для кристалів, вирощених різними методами, що свідчить про наявність відмінностей у механізмах утворення кластерів. В рамках моделей агрегації з обмеженою дифузією змодельовано утворення фрактальних структур на поверхні кристалів, вирощених з газової фази, та встановлено, що фрактальні кластери утворюються за механізмом "частинка–кластер", центрами росту в якому можуть служити неоднорідності структури поверхні кристала.